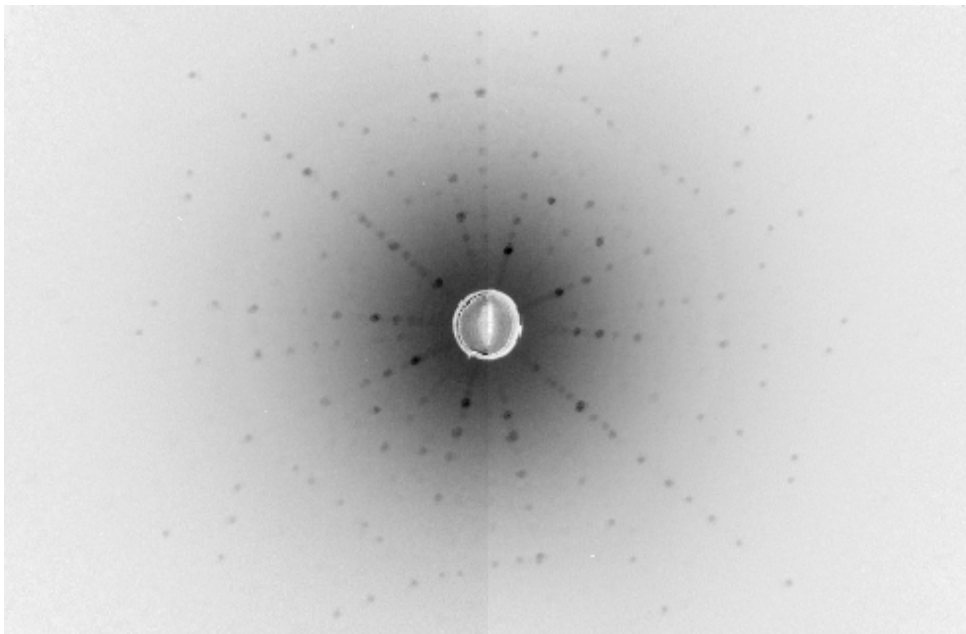


Advanced Laboratory Course

F69 – Laue X-ray Diffraction



INF 501, Room $\bar{1}03$

written by C. Neef, May 2015

(edited by K. Dey, W. Hergett, M. Jonak, S. Spachmann, August 2020)

TABLE OF CONTENTS

1	Introduction	3
2	Safety Instructions	4
3	Useful Resources	5
4	Preparation	6
5	Generation and Detection of X-Rays	7
5.1	Generation by X-Ray Tube	7
5.2	Detection of X-Rays	9
6	Single Crystal X-Ray Diffraction	11
6.1	Electron Density in Periodic Lattices	12
6.2	Structure Factors	14
6.3	Specifics of Laue Experiment	15
7	Crystal Structure and Stereographic Projections	16
7.1	Zones and Lattice Planes	16
7.2	Projections	16
7.3	Stereographic projections	17
8	Experimental Procedure	19
8.1	Goniometer	19
8.2	Automatic Psi-Circle Operation	21
8.3	High-Voltage Generator and X-Ray Tube Operation	21
8.4	Detector and Software	24
8.5	Analysis Software	25
9	Experimental Tasks	29
9.1	Silicon Wafer	29
9.2	Crystal of Your Choice	30
9.3	General Tasks	31
A	Appendix	32
A.1	Systematic Extinction of Reflexes	32
A.2	Generation of Stereographic Projections	33
B	Feedback	34

1 INTRODUCTION

How do atoms arrange in a material in order to form a crystal? This and many other fundamental questions are answered by crystallography and X-ray structure determination, which are invaluable tools for solid-state physics and many other natural and engineering sciences.

Whenever solid-state samples are subject of research, their structure analysis is the first step prior to determination of any other physical property. *X-ray powder diffraction* is capable of providing information, among others, about *lattice constants* and *bond angles*, and hence about symmetry and morphology of the particular species at hand.

On the other hand, *Laue X-ray diffraction* allows determination of the *crystal quality* of the sample at hand, thereby also providing information about grain sizes and the presence of defects. Moreover, Laue X-ray diffraction enables *orientation* of a single-crystalline sample; that is determination of the relation between the sample's crystallographic directions (the internal crystal lattice) and the laboratory system (the sample's external shape).

Whenever physical properties are expected to be anisotropic, the orientation of a single-crystalline sample is necessary in order to prepare it for further physical experiments. In practice, this may mean, for instance, aligning the sample with respect to a given laboratory direction along the sample's crystallographic [001]-axis in order to be able to measure physical properties along the *c*-axis in other experiments, such as magnetisation, electron spin resonance, resistivity, or thermal expansion and magnetostriction. The applications of Laue X-ray diffraction range from fundamental scientific questions to industrial testing procedures, such as quality assurance of semiconductor wafers or determination of material fatigue in turbine blades.

The aim of this laboratory course is to become acquainted with Laue X-ray diffraction. In particular, the following goals are envisaged:

1. to gain understanding of the relation between the crystal structure and X-ray diffraction patterns as seen in a Laue image;
2. to become familiar with typical Laue images, assessing them for their quality and for the quality of the underlying samples;
3. to obtain insight into how a single-crystalline sample of an unknown orientation can be oriented;
4. to become acquainted with diffraction data analysis and various crystallography software.

In order to achieve these goals, a silicon wafer is studied in the first, shorter part of the experiment, and a crystal of your choice in the second, longer part of the experiment. Furthermore, throughout the script, questions intended to deepen and cement your knowledge and understanding of the subject are provided.

Good luck and have fun!

2 SAFETY INSTRUCTIONS

Radiation protection and high-voltage generator

Participation in a radiation protection course is mandatory for participation in this laboratory course.

In the present course, a tungsten X-ray tube is used for generating X-rays with energy up to 55 keV. Exposition to this kind of ionising radiation can cause severe short- and long-term damage to biological tissue. For this reason, the X-ray tube is housed in a protective cabinet which must be closed whenever the tube is in operation. The high-voltage generator is connected to a number of safety switches which automatically switch the generator off whenever the cabinet doors are opened. However, this procedure is very rough and may cause damage to the X-ray tube and generator.

Experimental setup and detector

For your convenience, the X-ray tube, beam collimator, detector and goniometer tracks have already been appropriately aligned. Except for the goniometer, none of these components should be moved during the operation of the experiment, as their alignment may easily be lost and re-adjustment is time-consuming.

Owing to the high sensitivity of the scintillating X-ray detector layer used in this experiment, avoid any kind of contact with the layer. Scratching or even touching the layer may cause damage which could render the detector unusable.

Toxicity of samples

Depending on availability and choice, irritant or harmful samples may have to be handled within the laboratory course. Therefore, direct handling of samples should only be carried out in accordance with your supervisor. If necessary, protective gloves must be worn in order to avoid direct skin contact. Do not attempt to swallow or inhale the samples.

General conduct in the laboratory

Do not eat or drink in the laboratory.

Do not attempt to unplug the high-voltage power supply from the mains or manipulate it otherwise than prescribed in this manual.

Do not disassemble any parts of the experimental setup.

Do not handle unused X-ray tubes which are stored in the laboratory.

Avoid contact with the crystal cutter located in the corner of the laboratory.

3 USEFUL RESOURCES

The current manual does not give an exhaustive introduction to the science of crystallography and X-ray diffraction. Previous participation in a condensed matter physics course is highly recommended. If this is not the case, contact your supervisor in advance. A selection of books and websites to support your work is given below.

Useful printed resources:

- Elements of X-ray Diffraction – 3rd edition; B.D. Cullity and S.R. Stock; Pearson 2014.
- Kristallographie: Eine Einführung für Studierende der Naturwissenschaften – 9. Auflage; W. Borchardt-Ott and H. Sowa; Springer Verlag 2018.
- Moderne Röntgenbeugung – Röntgendiffraktometrie für Materialwissenschaftler, Physiker und Chemiker – 2. Auflage; L. Spieß et al.; Vieweg + Teubner 2009.
- Festkörperphysik – 1. Auflage; S. Hunklinger; Oldenbourg Wissenschaftsverlag 2007.
- Basic Concepts of Crystallography – 1st edition; E. Zolotoyabko; Wiley-VCH 2011.
- Basic Concepts of X-Ray Diffraction – 1st edition; E. Zolotoyabko; Wiley-VCH 2014.
- Introduction to Solid State Physics – 8th edition; C. Kittel; Wiley 2011.
- Solid State Physics – college edition; N.W. Ashcroft and N.D. Mermin; Harcourt 1976.

Useful online resources:

- Space-group tables:
<http://img.chem.ucl.ac.uk/sgp/large/sgp.htm>
- Lecture course on mineralogy:
<http://www.tulane.edu/~sanelson/eens211/index>
- CLIP – software for simulation of Laue patterns:
<http://clip4.sourceforge.net>
- VESTA – three-dimensional real-space visualisation software:
<http://jp-minerals.org/vesta/en>
- Stereographic projections:
<http://www.doitpoms.ac.uk/tlplib/stereographic/index.php>

4 PREPARATION

Before you start the practical work, you should have read this manual and be able to answer the following questions.

Crystal structure:

- Why do atoms arrange in a given way (crystal)? What is translational symmetry?
- What kinds of lattice systems are there and how do different Bravais lattices look?
- What symmetries does a cubic system possess?
- What is a crystal habit? How is it influenced by the crystal structure?

X-ray experiments:

- What are X-rays and how can they be generated? What is Bremsstrahlung?
- How can they be detected? How do they interact with matter?
- Why are they used to study crystal structures?
- What kinds of X-ray experiments do you know? What are they used for?
- What safety precautions must be taken while dealing with X-rays?

Laue X-ray diffraction

- What are the main differences between Laue X-ray diffraction and other types of X-ray diffraction experiments?
- What crystallographic information can and what crystallographic information cannot be obtained from a Laue experiment?
- What Laue image can be expected for (i) a single-crystal, and (ii) polycrystal sample?
- What effect on a Laue image can be expected for varying (i) X-ray tube voltage, and (ii) X-ray tube current?

Data analysis and evaluation:

- What is a stereographic projection? What does "angle-conserving" mean in the context of stereographic projections?
- What is a Wulff net?
- Why does the diffraction angle (angle between the incident and scattered beams) not depend on the lattice parameters in a cubic system? (Contradiction to Bragg's law?)

5 GENERATION AND DETECTION OF X-RAYS

X-rays are electromagnetic waves with photon energies of several keV. Their wavelength is in the range $0.1 \text{ \AA} \leq \lambda \leq 100 \text{ \AA}$, making them ideal candidates for diffraction experiments in solid state physics. Amongst many possible experiments, structure determination of crystals is one of the main applications of X-ray diffraction, as the X-rays' wavelength is of the same order as typical lattice constants. Structure determination can be achieved by the detection of monochromatic X-rays after interaction with the electronic shells of molecules or atoms inside a lattice.

Depending on the physical problem at hand, requirements for specific X-ray energy, spectral distribution and intensity can be very diverse. While high quality diffraction experiments rely on high intensity X-rays with a high degree of monochromaticity, the Laue experiment is carried out with polychromatic (i.e. "white") X-ray light. The following chapter describes the most common ways of X-ray generation and detection with specific attention to the techniques used in this experiment.

5.1 GENERATION BY X-RAY TUBE

The use of X-ray tubes is a common and rather inexpensive way of X-ray generation. The principle is based on electrons which are accelerated by a DC voltage and strike a metal target, whereby they lose their energy by interaction with the atomic cores in the metal. A typical setup consists of a cathode (C) and anode (A), which are located inside an evacuated glass tube (cf. Fig. 5.1). The heated cathode (U_h) ejects free electrons by thermionic emission, which are then accelerated towards the anode by a given DC voltage (U_a). The fast deceleration of the electrons during collision with the anode causes the emission of electromagnetic radiation. This kind of radiation is called Bremsstrahlung.

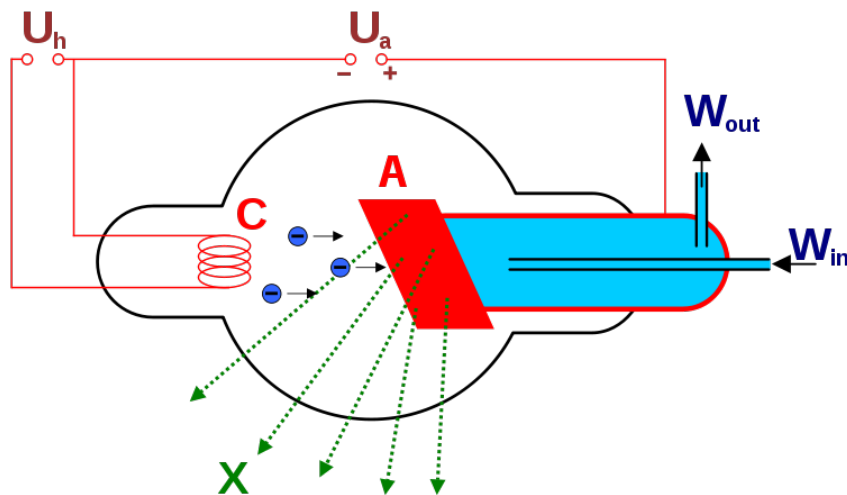


Figure 5.1: Principle of X-ray generation in an X-ray tube: Thermally (U_h) excited electrons are released from the cathode, C, and accelerated (U_a) towards the water-cooled (W_{in} , W_{out} ,) anode, A. The deceleration of the highly energetic electrons leads to the generation of X-ray photons (X). (From: public domain)

The Bremsstrahlung spectrum is schematically depicted in Fig. 5.2 and is given by Kramer's rule:

$$I(\lambda) \propto Z \left(\frac{\lambda}{\lambda_{\min}} - 1 \right) \cdot \frac{1}{\lambda^2} \quad (5.1)$$

where I is the spectral intensity, Z the atomic number of the anode material, and λ_{\min} the minimum wavelength (and thus the maximum energy) of a generated X-ray photon. The latter is determined by the kinetic energy of the electrons incident on the anode and thus by the acceleration voltage (U_a) applied between the cathode and anode:

$$E_{kin}^{electron} = e \cdot U_a = E_{max}^{photon} = \frac{2\pi\hbar c}{\lambda_{\min}} \quad (5.2)$$

It can be seen that the intensity increases with increasing acceleration voltage U_a and atomic number Z of the anode material.

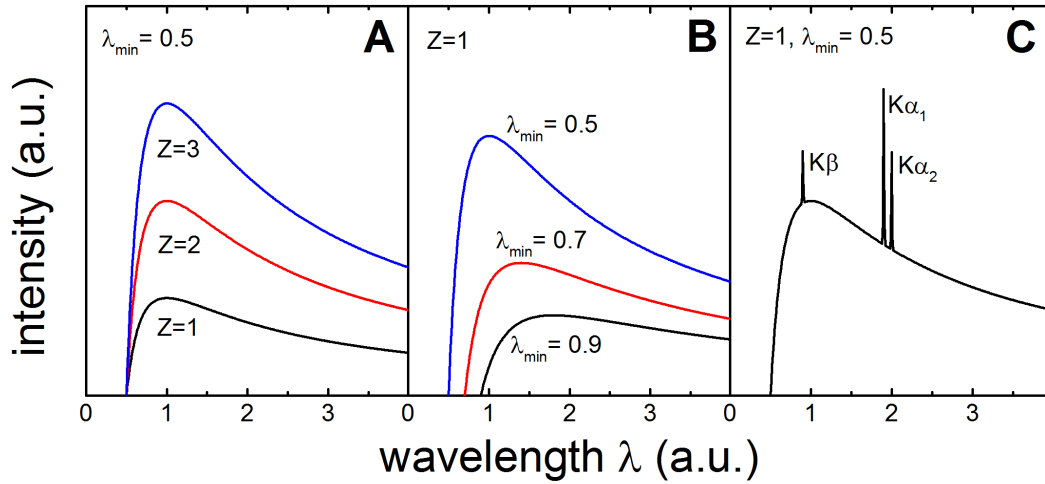


Figure 5.2: A schematic of X-ray spectra generated by an X-ray tube as a function of wavelength (A) for different atomic numbers Z of the anode; (B) for different minimum wavelengths λ_{\min} , and; (C) consisting of Bremsstrahlung and characteristic radiation.

In addition to the continuous intensity distribution of the Bremsstrahlung, narrow lines of high intensity, called characteristic lines, can appear at specific wavelengths. This happens if the electrons incident on the anode have high enough energy to eject an electron from one of the anode's inner electronic shells, leaving a hole in this shell. This hole can subsequently be filled with another electron from a higher-lying shell and the excess energy between both shells released by emission of an X-ray photon. Especially high-intensity characteristic lines are generated if the hole is created in the anode's inner K-shell. Table 5.1 lists the wavelengths of characteristic lines for some common anode materials.

As can be deduced from simple atomic models, the energy intervals between different atomic shells are proportional to Z^2 , leading to a quadratic increase in characteristic lines' X-ray energies for increasing atomic number of the anode. Fig. 5.2C shows a simple X-ray tube spectrum consisting of the continuous Bremsstrahlung spectrum and the characteristic lines. The relative linewidth

Element	Z	K_α Å(keV)	K_β Å(keV)
Co	27	1.79 (6.92)	1.62 (7.65)
Cu	29	1.54 (8.05)	1.39 (8.92)
Mo	42	0.71 (17.46)	0.63 (19.68)
W	74	0.21 (59.0)	0.18 (68.9)

Table 5.1: Characteristic lines for some typical anode materials.

of the characteristic radiation is of the order of $\Delta E/E \approx 10^{-4}$. Note that a real spectrum can be very complex and show various overlapping lines due to the large number of electronic states contributing to the characteristic emission and due to multi-step relaxation processes. In many diffraction experiments, only the $K\alpha_1$ line, exhibiting the highest intensity of all lines, is used. This line corresponds to an electronic transition from the $2p_{3/2}$ to the $1s$ state. For that purpose, special monochromators must be applied to filter out other characteristic lines and the continuum of the Bremsstrahlung.

Besides the right choice of anode material and acceleration voltage, X-ray tube design and electron beam focus have a great effect on the intensity of the generated X-rays. Generally, only 1% of the energy carried by the acceleration electrons is converted to X-rays at the anode, while the remainder is given off as heat. Additionally, most diffraction experiments require a well-collimated X-ray beam, thereby reducing the tube's efficiency still further. Given the above considerations, it comes as no surprise that the power input of a typical X-ray tube is several kW, whereas the X-ray output is in the order of one Watt.

A drastic increase in efficiency can be achieved by focusing the electron beam onto a small spot on the anode's surface. This is exploited in microfocus X-ray tubes in which an electron beam incident onto a spot size of $10\ \mu m$ to $100\ \mu m$ can increase the X-ray intensity hundred-fold in comparison to conventional tubes. The input power of such a system lies in the range of several W. Note however, that due to the high thermal load on the focus spot, the lifetime of microfocus tubes is relatively short.

5.2 DETECTION OF X-RAYS

The detection of X-rays can be achieved by photographic ex-situ techniques as well as in-situ cameras. Depending on the experiment and practical problem at hand, intensity, energy, and direction of the scattered X-ray photons have to be measured. In the following, the most common detection methods are presented.

Chemical processes and image plates

X-rays can be made visible in-situ by using either fluorescent films or films which change their chemical composition when irradiated. A prominent example for the latter is the use of ionic AgBr crystals pasted onto a photographic plate. An incident X-ray photon can break the Ag^+-Br^- bond, reducing Ag^+ to atomic silver. A crystal defect which darkens the photographic film is thereby generated. Despite the large number of other materials and techniques with different X-ray sensitivity, they all require a separate visualization or digitalization process, making in-situ observations impossible.

Counting tube

Counting tubes exploit the X-rays' ability to ionise atoms in a gas by building pairs of ions and electrons. Typical ionisation energies of gas molecules are in the range of 10 eV, allowing an X-ray photon with energy of several keV to ionise a great number of atoms. If a high DC voltage is applied over the gas volume, ions and electrons can be separated and lead to a current in the system, which can be used as a signal for measurement. In an ideal case, the strength of this signal is proportional to the energy of the X-ray photon. This principle can be extended by arranging several circuits in an array to form an area detector.

CCD cameras

For direct digital processing of the Laue data, the combination of a scintillating screen and a CCD camera can be utilised. In the present experiment, the conversion of X-ray photons to photons in the visible range is carried out by a scintillator material Gadox (Tb-doped $\text{Gd}_2\text{O}_2\text{S}$). The underlying process is the generation of electron-hole pairs in the material by the highly energetic X-ray photons that can then recombine by emission of visible light at the terbium activator. In case of Gadox, the wavelength of the emitted light is in the range $382 \text{ nm} \leq \lambda \leq 622 \text{ nm}$ with a maximum in the green region ($\approx 545 \text{ nm}$). The high mass density of Gadox and gadolinium's high atomic number are responsible for the strong scintillating properties of Gadox, making the material particularly suitable for X-ray detection.

CCD detectors can thereby yield high sensitivity due to high quantum efficiency and the small formation energy of electron-hole pairs as compared to the ionisation energy of gas molecules. A high spatial resolution given by the small pixel size and a comparably low cost can be achieved due to the industrial availability of CCD chips.

6 SINGLE CRYSTAL X-RAY DIFFRACTION

The following chapter gives a short introduction to the elastic scattering of X-rays as a result of their interaction with electronic shells in a periodic lattice. The concept of an incident monochromatic plane wave \mathbf{E}_i is used which is taken to scatter from a certain electron density $\rho(\mathbf{r})$. This electron density depends on the crystal structure of the underlying atomic lattice.

If a plane wave \mathbf{E}_i is elastically scattered from an electron at position \mathbf{r} , the electron itself becomes the source of a spherical wave \mathbf{E}_s . The two waves can be mathematically described as:

$$\begin{aligned}\mathbf{E}_i(\mathbf{r}) &= \mathbf{E}_0 \cdot \exp[-i(\omega_0 t - \mathbf{k}_0 \cdot \mathbf{r})] \\ \mathbf{E}_s(\mathbf{r}^*) &= \frac{\tilde{\mathbf{E}}}{r^*} \cdot \exp[-i(\omega_0 t - \mathbf{k}_0 \cdot \mathbf{r}^*)]\end{aligned}\tag{6.1}$$

where ω_0 is the angular frequency, \mathbf{k}_0 the wavevector, and \mathbf{E}_0 and $\tilde{\mathbf{E}}$ are the respective amplitudes. In case of several scattering centres or an electron density $\rho(\mathbf{r})$, the total scattered intensity follows from the overlap of all scattered waves. As can be seen in Fig. 6.1, these waves differ from each other by a certain phase shift. If the origin of the coordinate system is chosen to lie at one of the scattering centres, then the path difference between the wave scattered at the origin and at a volume element dV at position \mathbf{r} is given by $\delta s = \Delta S_1 + \Delta S_2 = (\mathbf{k} \cdot \mathbf{r})/k - (\mathbf{k}_0 \cdot \mathbf{r})/k_0$ when viewed from a detector in direction of \mathbf{k} (cf. Fig. 6.1). In the elastic limit, $k = k_0$, and δs becomes $((\mathbf{k} - \mathbf{k}_0)/k) \cdot \mathbf{r}$.

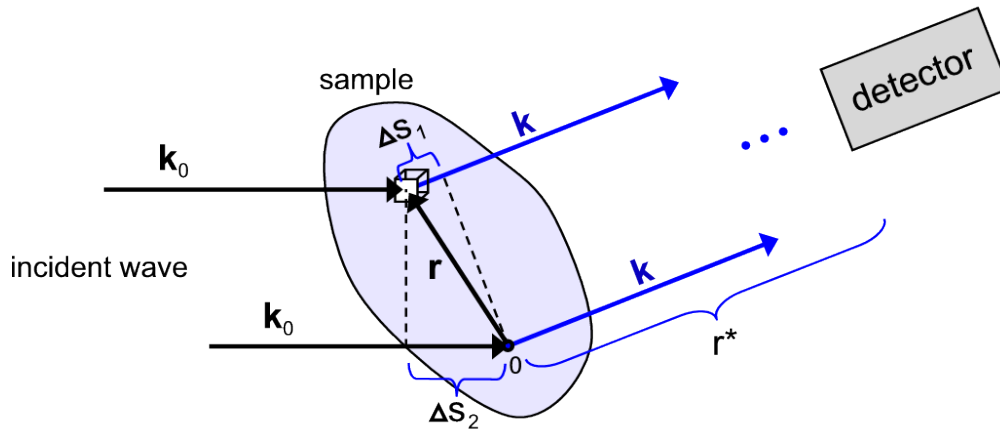


Figure 6.1: Principle of a diffraction experiment: An elastically scattered plane wave $k_0 \rightarrow k$ has a path difference $\delta s(\mathbf{r})$ which leads to a constructive interference or extinction measured by a detector. (From: *Festkörperphysik* – S. Hunklinger, Oldenbourg 2007)

The contribution from the volume element dV at position \mathbf{r} to the amplitude seen at the detector located at \mathbf{r}^* thus becomes:

$$dE_s = \rho(\mathbf{r}) \cdot E_s(\mathbf{r}^*)dV = \frac{\tilde{\mathbf{E}}}{r^*} \cdot \rho(\mathbf{r}) \cdot \exp[-i(\omega_0 t - \mathbf{k} \cdot \mathbf{r}^* + (\mathbf{k} - \mathbf{k}_0) \cdot \mathbf{r})]dV\tag{6.2}$$

and the integrated scattering amplitude of sample volume V :

$$E = \frac{\tilde{\mathbf{E}}}{r^*} \cdot \exp[-i(\omega_0 t - \mathbf{k} \cdot \mathbf{r}^*)] \int_V \rho(\mathbf{r}) \cdot \exp[-i((\mathbf{k} - \mathbf{k}_0) \cdot \mathbf{r})] dV \quad (6.3)$$

Eq. 6.3 can be identified with the Fourier transform of the electron density $\rho(\mathbf{r})$. If the scattering amplitude is measured, it should be possible to carry out a reverse Fourier transform in order to calculate this density and thus the atomic structure of the sample volume. This, however, is not possible, since only the intensity $I \propto |E|^2$ and not the amplitude itself can be measured. The accompanying loss of phase information is known in crystallography as the phase problem.

Luckily, one can still gather a lot of information just from the measured intensity. For a sample of known crystal structure $\rho'(\mathbf{r})$, it is possible to compare the measured intensity with the calculated intensity I' , derived from $\rho'(\mathbf{r})$, in order to obtain information about the crystallinity and orientation of the sample. This method of understanding Laue images is employed also in the current experiment by way of analysing the experimental data with CLIP (cf. Section 8).

For a sample of unknown crystal structure, it is possible to search for a matching intensity pattern in crystal structure databases. Similar structures can offer a good starting point to construct a model to describe the experimental data. Another possibility for samples of unknown crystal structure is to solve the structure solely by trial-and-error methods. In that case, complex numerical algorithms, such as "charge-flipping algorithm" (CFA), are used to find a matching structure starting from a completely random density $\rho'(\mathbf{r})$. The convergence of such procedures is strongly dependent on the quality of the data, which in turn is dependent on the sample quality as well as the experimental procedure.

6.1 ELECTRON DENSITY IN PERIODIC LATTICES

After discussing general scattering at an unspecified charge density $\rho(\mathbf{r})$, the special case of scattering at an ordered crystal lattice is considered in the following. The periodicity and symmetry of the lattice $\rho(\mathbf{r}) = \rho(\mathbf{r} + \mathbf{R})$, with $\mathbf{R} = u\mathbf{a}_1 + v\mathbf{a}_2 + w\mathbf{a}_3$ being a lattice vector (where u, v, w are integers), is used to expand the charge density in a Fourier series:

$$\rho(\mathbf{r}) = \sum_{h,k,l} \exp(i\mathbf{G}_{hkl} \cdot \mathbf{r}) \quad (6.4)$$

where \mathbf{G} is a reciprocal lattice vector and h,k,l are integers. From translation invariance $\exp(i\mathbf{G}_{hkl} \cdot \mathbf{r}) = \exp(i\mathbf{G}_{hkl} \cdot (\mathbf{r} + \mathbf{R}))$ it follows directly that $\mathbf{G}_{hkl} \cdot \mathbf{R} = 2\pi p$, with p being an integer, which is exactly the definition for the reciprocal lattice.

If a scattering vector $\mathbf{K} = \mathbf{k} - \mathbf{k}_0$ is introduced, the scattering intensity can be written as:

$$|A(K)|^2 = \left| \sum_{h,k,l} \rho_{hkl} \int_V \exp[i(\mathbf{G} - \mathbf{K}) \cdot \mathbf{r}] \right|^2 \quad (6.5)$$

It can be seen that the integral over an infinitely large volume V vanishes because of the oscillating character of the exponential function. Hence, the scattered intensity will be cancelled out in all

directions that do not fulfil the condition $\mathbf{G} - \mathbf{K} = 0$. In case of crystal volumes which are large compared to the unit cell, a finite scattering intensity will thus only be observed if the X-ray beam (given by \mathbf{k}_0), the crystal's reciprocal lattice vector \mathbf{G}_{hkl} and the detector's position (direction of \mathbf{k}) fulfil the condition $\mathbf{k} - \mathbf{k}_0 = \mathbf{G}_{hkl}$ for a specific set of integers h, k, l .

It goes without saying that in real experiments, the measured scattered intensity will be influenced by additional parameters. Firstly, the source will show some degree of polychromaticity ($\mathbf{k} \neq \text{const}$) and beam divergence; secondly, small crystallite sizes or finite penetration depths of X-rays, as well as thermal movement of atoms will lead to a broadening of scattered reflection peaks or loss of intensity.

The scattering condition can be visualised with the so-called Ewald sphere (see Fig. 6.2A) which allows to find all reciprocal vectors for which the elastic scattering condition $|\mathbf{k}| = |\mathbf{k}_0|$ is satisfied (the radius of the Ewald sphere is given by $|\mathbf{k}_0|$). In Fig. 6.2A, the condition is fulfilled only for the reciprocal vectors $G = (310)$ and $G = (5\bar{6}0)$, and hence, constructive interference can be measured only along (310) and $(5\bar{6}0)$.

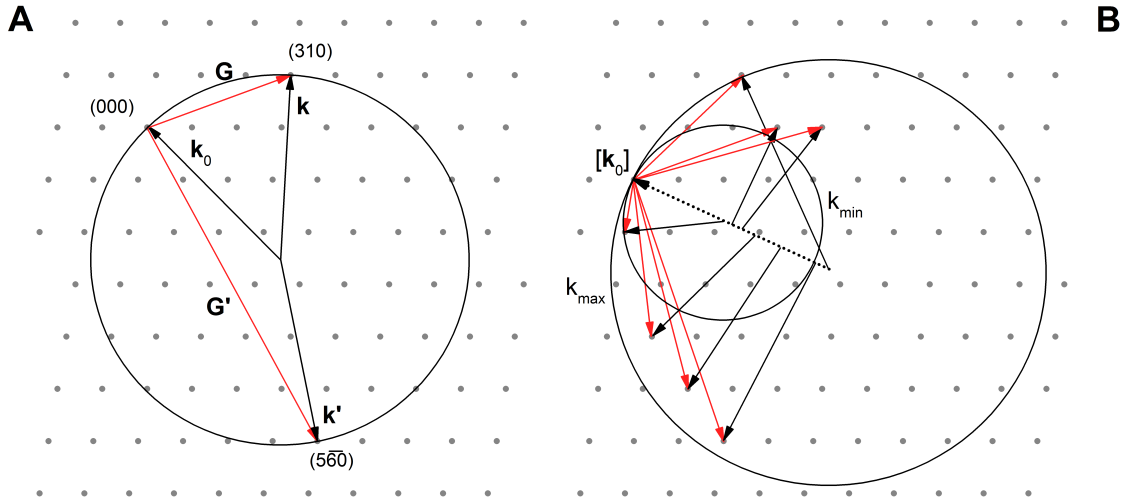


Figure 6.2: Ewald sphere representing the scattering condition $\mathbf{G} - \mathbf{K} = 0$ (A) for monochromatic X-rays k_0 ; (B) for polychromatic X-rays with $k_0 \in [k_{\min}, k_{\max}]$.

Additionally, with

$$d_{hkl} = 2\pi / |\mathbf{G}_{hkl}| \quad (6.6)$$

where d_{hkl} is the interplanar distance, i.e. the perpendicular distance between two successive planes from a family of planes $\{hkl\}$, and with

$$|\mathbf{K}| = |\mathbf{k} - \mathbf{k}_0| = 2k_0 \sin(\theta) = 4\pi \sin(\theta) / \lambda \quad (6.7)$$

where θ is one half of the angle between \mathbf{k} and \mathbf{k}_0 (i.e. 2θ is the diffraction angle), and λ is the wavelength of the incident X-ray beam, the scattering condition can be transformed into the famous Bragg's law:

$$2d_{hkl}\sin(\theta) = \lambda \quad (6.8)$$

A complementary description of elastic scattering in periodic lattices can be given by the so-called Laue equations. Bearing in mind the scattering condition $\mathbf{G} - \mathbf{K} = 0$ and exploiting the relation $\mathbf{b}_i \cdot \mathbf{a}_j = 2\pi\delta_{ij}$, the scalar product of $\mathbf{G} = h\mathbf{b}_1 + k\mathbf{b}_2 + l\mathbf{b}_3$ with the real-lattice vectors \mathbf{a}_i yields the three Laue equations:

$$\begin{aligned} (\mathbf{k} - \mathbf{k}_0)/|\mathbf{k}| \cdot \mathbf{a}_1 &= \lambda h \\ (\mathbf{k} - \mathbf{k}_0)/|\mathbf{k}| \cdot \mathbf{a}_2 &= \lambda k \\ (\mathbf{k} - \mathbf{k}_0)/|\mathbf{k}| \cdot \mathbf{a}_3 &= \lambda l \end{aligned} \quad (6.9)$$

Since $\mathbf{k}/|\mathbf{k}|$ and $\mathbf{k}_0/|\mathbf{k}|$ are known or measured during the experiment, h, k, l can be deduced from the lattice constants. Each of the three equations in 6.9 can be visualised as a cone, the so-called Laue cone. For that, we consider the condition on \mathbf{k} for which constructive interference can be observed. At a fixed wavelength and setup geometry, \mathbf{k}_0 and \mathbf{a}_i are constant, and hence for a particular lattice plane (hkl), each of the Laue equations in 6.9 can be written as:

$$\mathbf{k} \cdot \mathbf{a}_i = \text{const.} \quad (6.10)$$

or

$$\cos(\alpha) \cdot k \cdot a_i = \text{const.} \quad (6.11)$$

where α is the angle between \mathbf{k} and \mathbf{a}_i . In order to observe constructive interference on a detector, all three Laue equations must be fulfilled at the same time, i.e. \mathbf{k} must point to the intersection of the three Laue cones generated by the three Laue equations in 6.9. For a polychromatic X-ray beam, the Laue equations predict a continuum of Laue cones, whose limits are given only by the lower and upper wavelength bounds of the incident radiation (see Section 5). Consequently, a large number of three-Laue-cones intersections and thus intensity spots on the screen are predicted for any kind of crystal orientation.

6.2 STRUCTURE FACTORS

Whereas the general scattering condition $\mathbf{G} - \mathbf{K} = 0$ can be derived solely from the translational symmetry of the lattice, further symmetry elements and atomic properties will also affect the measured diffraction intensities and may cause disappearance of certain diffraction peaks otherwise allowed on the basis of the arguments presented thus far. These further factors have so far been incorporated into the Fourier coefficients ρ_{hkl} . They are mathematically given by:

$$\rho_{hkl} = \frac{1}{V_Z} \cdot \int_{V_Z} \rho(\mathbf{r}) \cdot \exp[-i(\mathbf{G}_{hkl} \cdot \mathbf{r})] dV \quad (6.12)$$

where V_Z is the unit cell volume. A crystal's electronic density $\rho(\mathbf{r})$ is determined by atoms' positions within the unit cell, as well as by the internal structure of the individual atoms making

up the crystal, e.g. their electronic shells. The latter is further quantified by the so-called atomic structure factor f_{atom} and can be calculated or deduced from collision experiments. In practical diffraction analysis, f_{atom} is not refined from the experimental data, but merely taken from crystallographic tables, since the approximation of scattering centres as free atoms is often sufficient for a satisfactory interpretation of diffraction patterns.

On the other hand, the positions of individual atoms in the unit cell do have a crucial influence on the diffraction patterns, as they lead to additional interference between X-ray beams scattered by different atoms. If this kind of distinction between atomic positions and atomic structure factor is made, Eq. 6.12 can be written as:

$$\rho_{hkl} = \frac{1}{V_Z} \sum_{\text{base}} \exp[-i(\mathbf{G} \cdot \mathbf{r}_{\text{atom}})] \int_{V_{\text{atom}}} \rho_{\text{atom}}(\mathbf{r}^*) \cdot \exp[-i(\mathbf{G} \cdot \mathbf{r}^*)] dV \quad (6.13)$$

which results in

$$\rho_{hkl} = \frac{1}{V_Z} \sum_{\text{base}} f_{\text{atom}}(G) \cdot \exp[-i(\mathbf{G} \cdot \mathbf{r}_{\text{atom}})] \quad (6.14)$$

where \mathbf{r}_{atom} are individual atomic positions and the sum is performed over all atoms in the unit cell. Eq. 6.14 can be simplified if the positions \mathbf{r}_{atom} are written in terms of the unit cell vectors $\mathbf{r}_{\text{atom}} = u\mathbf{a}_1 + v\mathbf{a}_2 + w\mathbf{a}_3$, and the relations between \mathbf{G} and \mathbf{R} are used:

$$\rho_{hkl} = \frac{1}{V_Z} \sum_{\text{base}} f_{\text{atom}}(G) \cdot \exp[-2\pi i(hu + kv + lw)] \quad (6.15)$$

Dictated by the atomic positions and symmetries of the crystal, ρ_{hkl} vanishes if the terms inside the sum cancel each other out. An overview of several crystal symmetries and cancellation of reflexes is given in the appendix.

6.3 SPECIFICS OF LAUE EXPERIMENT

While for the derivation of the scattering theory developed thus far, a monochromatic X-ray source ($|\mathbf{k}_0| = \text{const.}$) has been assumed, the situation in a Laue setup is different. Here, a polychromatic or "white" X-ray source is used, and thus the scattering condition is fulfilled for many different reflexes at the same time. Nevertheless, the concept of an Ewald sphere can still be used for visualising the experimental conditions. In contrast to a monochromatic scenario with one Ewald sphere, we now find a volume between two Ewald spheres of radius k_{min} , and k_{max} , respectively, inside of which all reciprocal lattice points will lead to constructive interference at the same time (see Fig. 6.2B). Note that k_{min} (or λ_{max}) is given by the decreasing intensity of Bremsstrahlung for higher wavelengths and k_{max} (or λ_{min}) by the acceleration voltage.

The benefit of this method is obvious: if an area detector is used, a lot of different reflexes can be seen at the same time and the orientation and symmetry deduced immediately. Nevertheless, advanced crystal structure analysis cannot be carried out by this method, since almost all the information which is carried by the reflex intensity is lost due to the variation of intensity of the produced X-rays with their wavelength.

7 CRYSTAL STRUCTURE AND STEREOGRAPHIC PROJECTIONS

The following section discusses aspects of crystallography pertinent to Laue diffractometry.

7.1 ZONES AND LATTICE PLANES

Real-space straight lines in a lattice can be represented by linear combinations of the unit cell vectors \mathbf{a}_i : $\mathbf{x} = u\mathbf{a}_1 + v\mathbf{a}_2 + w\mathbf{a}_3$ or simply by a vector $[uvw]$. Note that $[uvw]$ does not only represent the straight line between the origin and \mathbf{x} but also any parallel line within the translation invariance of the lattice. Two non-parallel lattice vectors $[u_1v_1w_1]$ and $[u_2v_2w_2]$ span a unique lattice plane which can be denoted by a vector with Miller indices (hkl) orthogonal to the lattice plane. These indices follow from the zone equations:

$$\begin{aligned} h \cdot u_1 + k \cdot v_1 + l \cdot w_1 &= 0 \\ h \cdot u_2 + k \cdot v_2 + l \cdot w_2 &= 0 \end{aligned} \tag{7.1}$$

Note again that (hkl) does not represent only one plane but a family of all parallel lattice planes with separation $n \cdot d_{hkl}$, where n is an integer. Conversely, the intersection of two planes $(h_1k_1l_1)$ and $(h_2k_2l_2)$ gives a lattice vector $[uvw]$ following:

$$\begin{aligned} u \cdot h_1 + v \cdot k_1 + w \cdot l_1 &= 0 \\ u \cdot h_2 + v \cdot k_2 + w \cdot l_2 &= 0 \end{aligned} \tag{7.2}$$

Since the assignment of lattice vectors and planes is not unique, the term "zone axis" $[uvw]$ is used to describe the family of planes $(h_ik_il_i)$ which all contain the axis $[uvw]$. Note that a zone $[uvw]$ is represented as a vector in real space but as a plane (containing all reciprocal vectors $(h_ik_il_i)$) in reciprocal space. And vice versa, a real-space lattice plane (hkl) containing all perpendicular vectors $[u_iv_iw_i]$ is represented as a vector in reciprocal space.

7.2 PROJECTIONS

One of the challenges in interpreting Laue images is the distortion which occurs when a spherical, three-dimensional diffraction pattern is recorded on a flat, two-dimensional detector. The information contained in a Laue image are the angles between various constructively interfering X-ray beams, whereby each individual beam originates from a unique family of $\{hkl\}$ planes. Upon hitting the detector, this angular information becomes encoded into distances between different spots. The spots are found to be located on specific curves which arise from the intersection of a cone with the plane of the detector (see Fig. 7.1A).¹ Each such cone itself is formed by all beams diffracting from the set of planes which revolve around a common axis, the zone axis. In the back-scattering geometry, the curves on which the spots lie are straight lines or hyperbolae

¹This cone is not to be confused with the Laue cone. See the ensuing discussion and also Section 6.1

(Fig. 7.1B), whereas in the forward-scattering, transmission geometry, the curves are generally ellipses or hyperbolae (Fig. 7.1C).

Another approach comes from the opposite direction: If the crystal structure is known, a simulated Laue pattern can be generated and compared with the measured pattern. Especially for complex lattices, the use of suitable software can be very helpful to obtain the orientation in a short time. This method is also used in the present laboratory course to find the orientation of various single-crystalline samples.

There are several possibilities how to find angles between different zone axes and thus the orientation of a crystalline sample. One is simply by calculating and transforming the zone-dependent reflections from the laboratory system into the crystal system. Although processing this by hand can be very time-consuming, pen-and-paper methods have been developed to solve this problem in a graphical way, e.g. by means of a "Greninger chart". This is an easy tool to obtain meridian and parallel coordinates of spots, similar to coordinates on the globe.

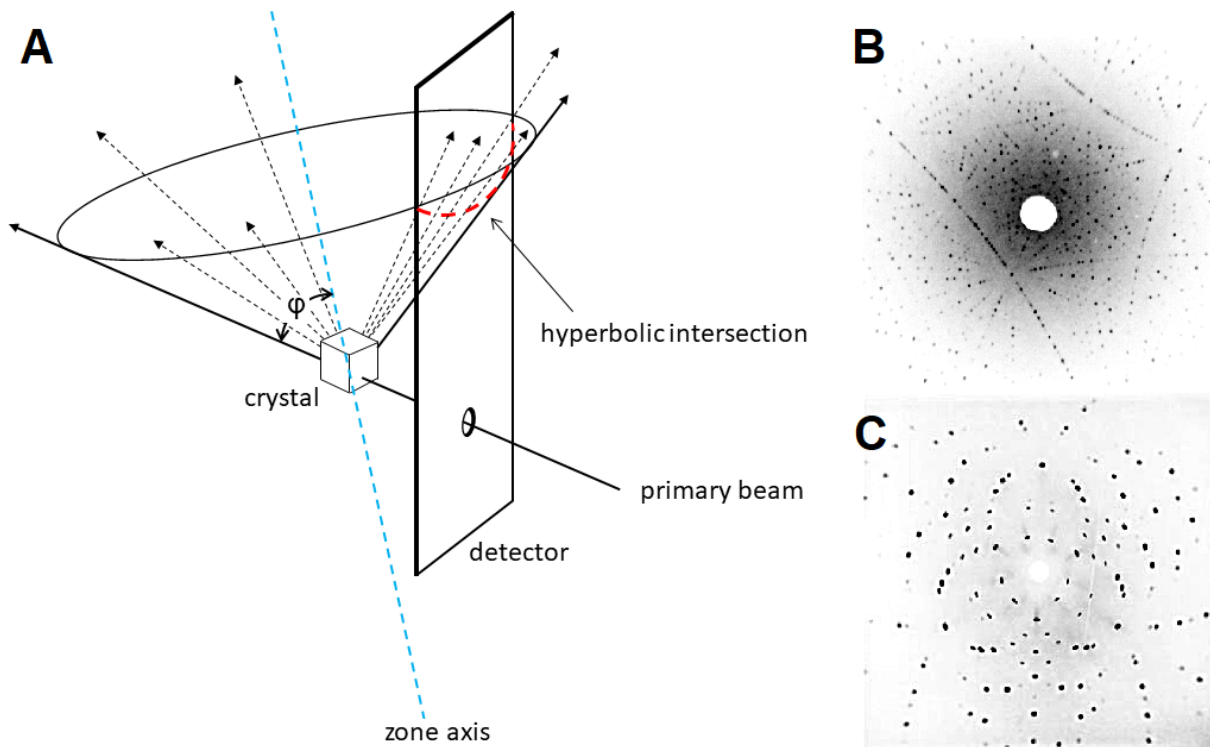


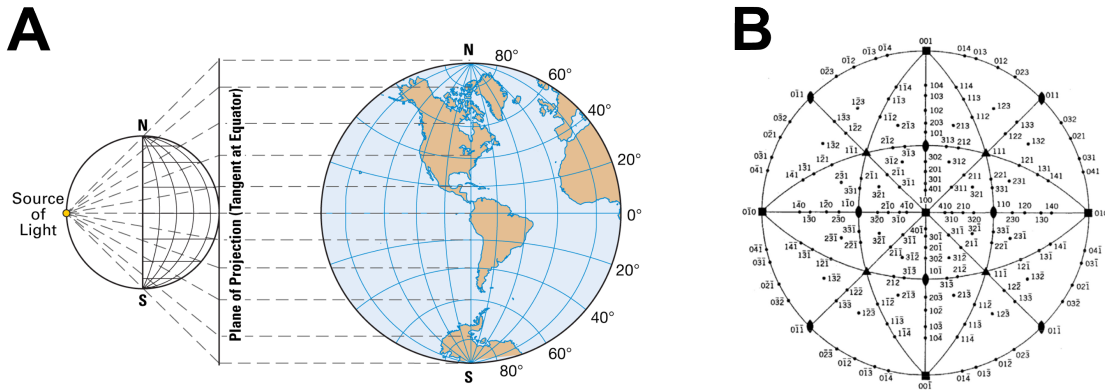
Figure 7.1: A: Principle of a back-scattering Laue experiment: A cone of constructively interfering beams reflecting from a crystal's particular zone propagates through space and is incident on a two-dimensional detector. The thus-generated spots lie on a hyperbola. One side of the cone is tangent to the transmitted beam, and the angle of inclination of the zone axis to the transmitted beam, ϕ , is equal to the semiapex angle of the cone; B: Back-scattering Laue image of an arbitrarily oriented LiMnPO_4 single crystal; C: Forward-scattering Laue image of a silicon crystal oriented in the (111) direction.

7.3 STEREOGRAPHIC PROJECTIONS

Plotting the diffraction spots as a stereographic projection is a helpful tool for finding the crystal orientation. The word "stereographic" denotes the projection of a three-dimensional object onto a two-dimensional plane, as it is for example done with two-dimensional images of the globe

(see Fig. 7.2A). A stereographic projection is angle-preserving; i.e. angular differences between diffraction spots do not change if the direction of the projection is changed. Fig. 7.2B depicts the standard stereographic projection of a cubic crystal in the (100) direction (corresponding to 0°). The (010) and (001) faces are perpendicular to the viewing direction and hence can be found on the poles of the circle lying in the plane of the screen (corresponding to 90°).

Similarly to the globe, the position on a stereographic projection can be given by longitude (Längengrad, δ) and latitude (Breitengrad γ). The so-called Wulff net will be used also during this laboratory course to find relative angles between different lattice planes of a crystal.



8 EXPERIMENTAL PROCEDURE

A schematic sketch of the setup is depicted in Fig. 8.1: a high-voltage generator (Kristalloflex 710 H, Siemens) is connected via a high-voltage cable to a tungsten X-ray tube (Bruker). A beam of X-rays leaves the X-ray tube through a beryllium window, passes the detector through a collimator located in the middle of the detector screen, and is scattered by the sample. The diffraction image is taken by the detector in a back-scattering geometry. The data acquisition and analysis are performed on a computer. Throughout operation, the high-voltage generator and the X-ray tube are water-cooled.

In the following, the functioning and operation of individual components of the experimental setup are described in detail.

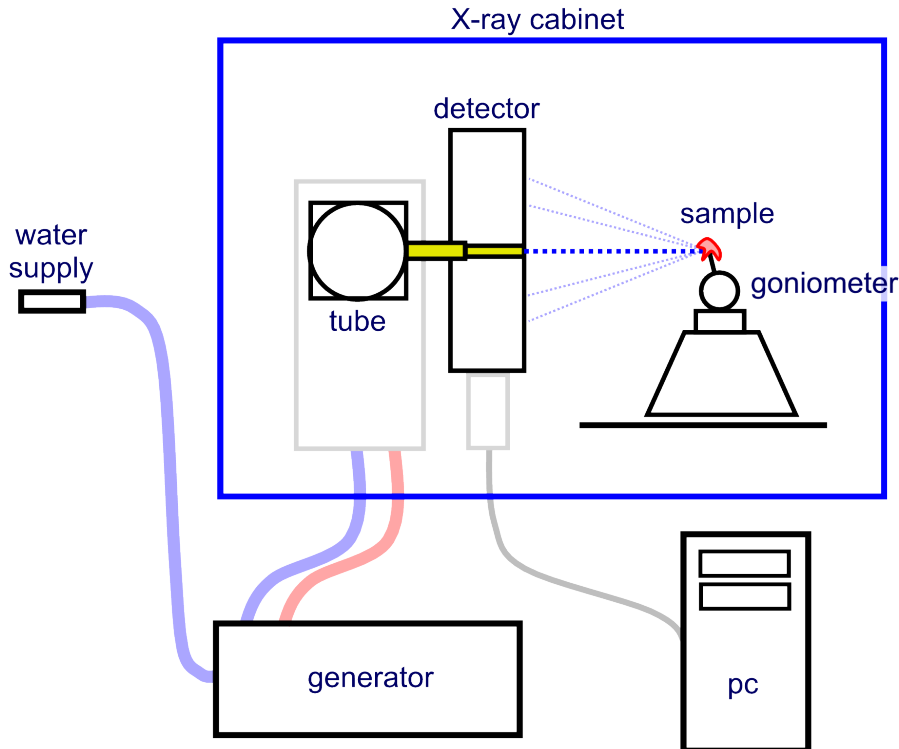


Figure 8.1: Schematic sketch of the experimental setup. The X-ray tube and beamline are housed inside a safety cabinet.

8.1 GONIOMETER

In general, single-crystal samples may not have a regular shape since they may have cracked or been broken off from larger pieces (e.g. rocks or polycrystalline fabric). Without any hints at visible external faces, a sample has to be rotated around three non-collinear axes in order to get it into the desired orientation (e.g. the (100) direction).

In this experiment a goniometer is used which allows, on the one hand, for the orientation of the

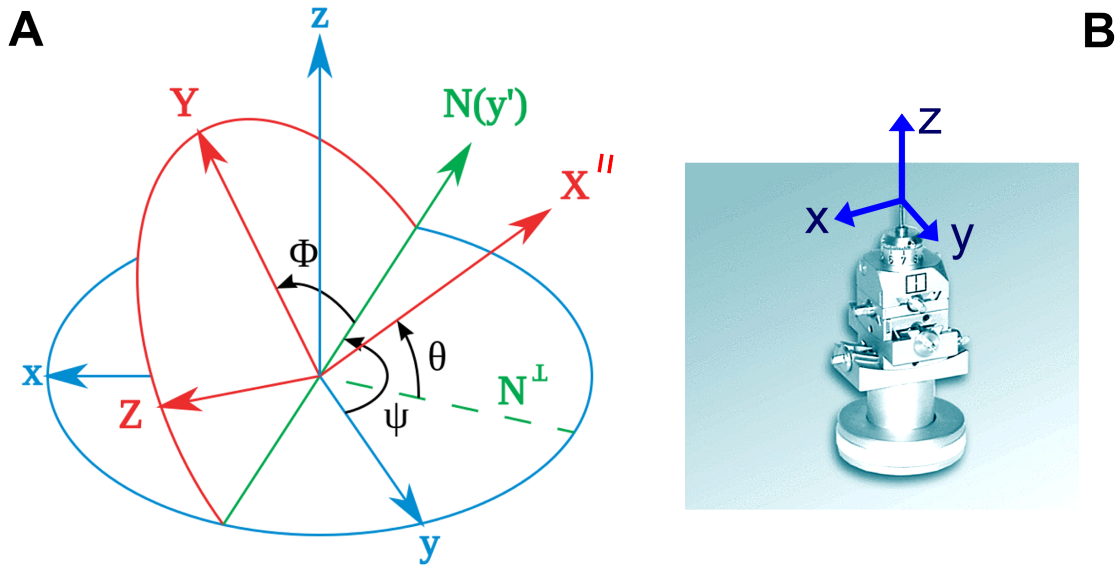


Figure 8.2: A: Coordinate transformation by z, y', x'' convention (1. Ψ , 2. θ , 3. Φ rotation) (From: public domain); B: Goniometer employed in the experiment, together with its coordinate system.

sample using three Euler's angles, and, on the other hand, for a linear translational motion of the sample in three directions.

The angular system used for this kind of goniometer follows the z, y', x'' convention and is called yaw (Gier), pitch (Nick), roll (Roll) system. These names originate from automotive engineering. Fig. 8.2A shows the procedure of achieving a specific orientation. The starting coordinate system (x, y, z) correlates with the laboratory system (cf. Fig. 8.2B). Firstly, the sample, which is positioned at the origin of the coordinate system, is rotated around the z -axis (Ψ -rotation). Thereby, the x - and y -axes are transformed to x' - and y' -axes. The next rotation is made around the new y' -axis (θ - or $R_{y'}$ -rotation), giving new x'' - and z'' -axes. The last rotation (Φ or $R_{x''}$) is around the x'' -axis and gives the final coordinate system, $X = x'', Y, Z$ (depicted red in Fig. 8.2A).

The option of linear translation is implemented in the upper part of the goniometer, hence leaving the angular rotations made by the $\Psi, R_{y'}, R_{x''}$ rotations intact. It can be considered as a linear shift within the final, red coordinate system: $X \rightarrow X + \Delta X, Y \rightarrow Y + \Delta Y, Z \rightarrow Z + \Delta Z$.

The last free parameter in the experimental setup is the distance between the sample and the detector screen which can be adjusted by moving the goniometer column on a linear rail. In order to ease the data analysis, this distance should be kept fixed for all measurements. For this purpose, a conical metallic spacer is suspended from the top of the detector's screen, enabling a fast adjustment. One of the experimental tasks is to ascertain what this distance is in the present experimental setup. Special care needs to be taken when handling the spacer in order not to touch the detector's surface.

8.2 AUTOMATIC PSI-CIRCLE OPERATION

The goniometer base is rotatable by an automatic step drive. This corresponds to a Ψ -rotation of the goniometer around the z -axis. The step drive can be operated even when the X-ray tube is running, which enables to take images of different sample orientations without having manually to touch the sample or goniometer. The drive can be controlled on the panel next to the PC. After the controller has been turned on (red on/off switch), the electronics should be reset by switching the three-position I/0/II switch to "0" for a few seconds and then back to position "II". Subsequently, the drive can be activated by pressing the enable switch. Pressing in the direction switch inverts the direction of rotation.

Before using the automatic drive, make sure that no part of the goniometer can come into contact with the detector as the goniometer is rotated.

8.3 HIGH-VOLTAGE GENERATOR AND X-RAY TUBE OPERATION

The generator used in this experiment is capable of applying high voltage between 20 kV and 55 kV at an X-ray tube current between 5 mA and 40 mA, resulting in a maximal power output of approximately 2.2 kW. However, due to low efficiency of the X-ray tube used in this experiment and as already discussed in Chapter 5, most of the input power is converted into heat. To cool off the waste heat, both, the generator and the X-ray tube are connected to cooling water. In order to operate the generator, the water valve must be completely opened. The flow can be checked at the flow meter and a minimum flow rate of 4.5 l/min must be observed. It is possible that the water pipes will feel (lukewarm) when the valve has just been opened for the first time on a given day. If this is the case, before you operate the high-voltage generator, let the cooling water run until you can feel the pipes are cool (ca. ten minutes).

To protect the X-ray tube from damage, the high voltage across it must be ramped up and down slowly. Depending on the tube's history, there are specific retention times – dwell times – for which the voltage must be kept constant before proceeding with the ramp-up. Table 8.1 displays the dwell times in dependence of the standstill time for which the X-ray tube has not been used. Consult the laboratory notebook for the last operation of the tube. As an example, if the tube has not been used for five days and voltage of 35 kV is to be applied, the ramp-up must occur in four steps: (i) starting at the minimum voltage of 20 kV and minimum current of 5 mA followed by 120 s of waiting; (ii) slow increase of the voltage to 25 kV followed by 120 s of waiting; (iii) slow increase to 30 kV followed by 180 s of waiting; (iv) slow increase to 35 kV followed by 180 s of waiting. After this procedure, the current can be adjusted to the desired level. This should also be done in steps of 10 mA with a dwell time of 120 s between each step.

Standstill (days)	Dwell time (min)			
	20kV	25kV	30kV	35kV
<3	2	2	2	2
3 to 30	2	2	3	3
>30	2	2	3	3

Table 8.1: X-ray tube dwell times to be observed during ramping-up of the high voltage based on the number of days for which the tube has been in a standstill.

The tube's cathode is heated with current between 1.9 A and 2.9 A, resulting in power input of up to 50 W. The generator's display is preset to show the X-ray tube current in mA. The X-ray tube voltage (in kV) and the cathode heating current (in A) can be read off by pressing the black buttons "kV" and "A", respectively (cf. Fig. 8.3).

In order to ensure safe operation of the system, do not exceed the X-ray tube current of 20 mA and voltage of 35 kV. In order to extend the system's lifetime, minimise the amount of time for which the high voltage is on. The X-ray tube can and must only be operated if the protection cabinet is properly closed. In order to protect the tube and generator, do not open the cabinet during X-ray operation. Lastly, unnecessary starting and stopping of the high-voltage generator should be avoided at all times.

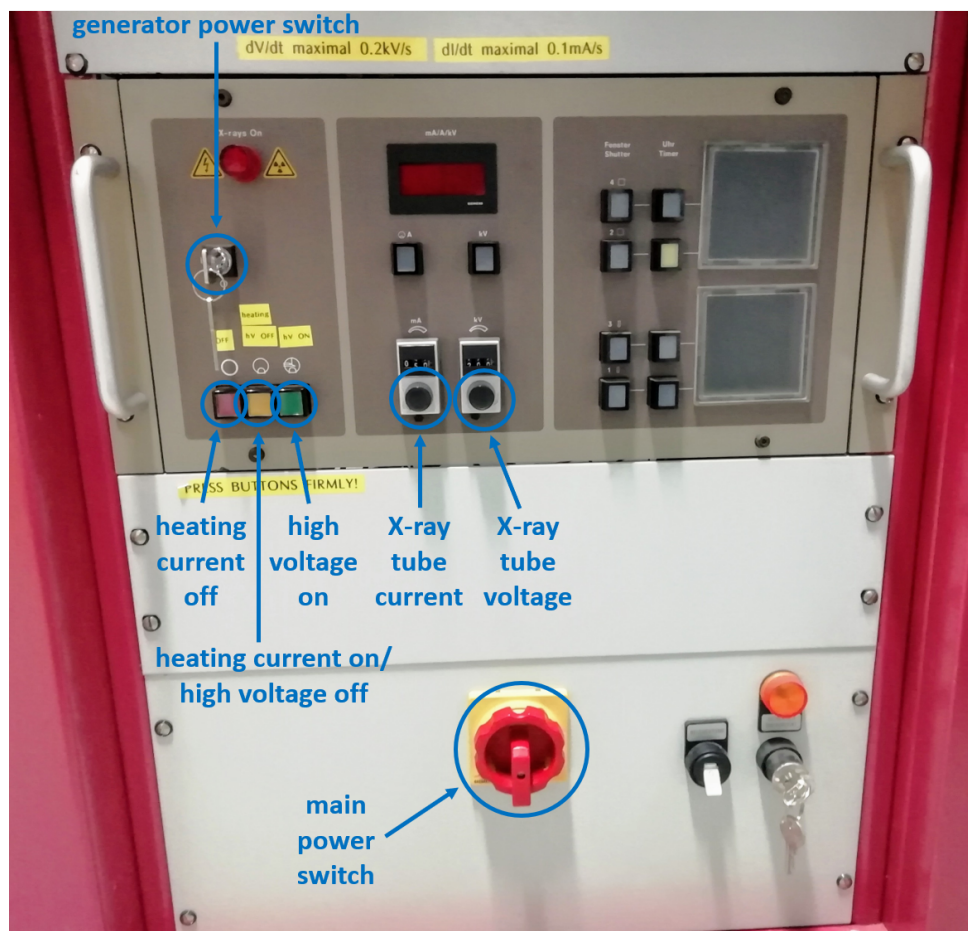


Figure 8.3: Front panel of the high-voltage generator.

To operate the experimental setup, follow these steps (cf. Fig. 8.3):

1. Turn on external cooling-water supply, check water flow and feel the pipes' temperature. You should be able to hear the water running through the X-ray tube;
2. Place your sample in the desired position onto the goniometer;
3. Set controllers for X-ray tube current and voltage to minimum (5 mA, 20 kV);

4. Turn on main power switch. Note that the main power switch controls the power to all electronics in the setup, including the high-voltage generator, detector, and computer;
5. Turn on the generator power switch key (Position "1");
6. Press orange button ("Heating") and wait for 120 s before proceeding further. You should be able to hear a periodic whizzing of the cooling fan coming from the right-hand side of the cabinet;
7. (At the latest now) shut cabinet doors;
8. Press green button ("hV ON") to start X-ray emission. You should be able hear a continuous buzzing of the transformer coming from the back of the cabinet;
9. Adjust the high voltage to desired level in accordance with Table 8.1 using the high-voltage controller ("kV"). Observe the maximum ramp-up rate of 0.2 kV/s;
10. Adjust the X-ray tube current to desired level using the current controller ("mA"). Observe a 120-second dwell time after each ramp-up of 10 mA. Observe the maximum ramp-up rate of 0.1 mA/s.

The tube is now running and detector images can be taken using the software, as described below. The shut-down procedure is as follows:

1. Using the appropriate controller, decrease the X-ray tube current to the minimum of 5 mA. Observe the maximum ramp-down rate of 0.1 mA/s (no need to observe the 120-second dwell times);
2. Using the appropriate controller, decrease the X-ray tube voltage to the minimum of 20 kV. Observe the maximum ramp-down rate of 0.2 kV/s (no need to observe the dwell times listed in Table. 8.1);
3. Press the orange button ("hV OFF"). The high voltage is now off and it is safe to open the cabinet doors;
4. In order to switch the heating current off, press the red button ("OFF"). This should only be done at the end of the experiment.

Should any other sounds than those described above, or a smell of burning develop during the operation of the experiment, immediately shut down the setup following the above shut-down procedure and contact your supervisor.

At the end of the day or experiment, the generator and complete system (PC, detector) are to be shut down with the generator power switch and the main power switch. Lastly, the cooling-water valve is to be closed.

8.4 DETECTOR AND SOFTWARE

The detector used in this experiment consists of two separate CCD chips, each with 1392×1040 pixels and active area of $85 \text{ mm} \times 110 \text{ mm}$. The incident X-ray beam passes the detector through an opening between both chips. Each pixel is read out by an A/D converter giving a twelve-bit intensity value. To minimise noise by stray radiation, both CCDs are placed inside a black box. The front side is covered with a capton layer which is impermeable to visible light but transparent to X-rays. The scintillating Gadox layer and the subsequent optics are placed directly in front of the CCD chips. Furthermore, thermal noise is reduced by cooling the chips with two peltier elements to $-10 \text{ }^{\circ}\text{C}$. In order to ensure proper cooling, the detector should be switched on 20 minutes prior to image acquisition. The power supply is activated automatically by turning on the main power switch (see Fig. 8.3).

The image read-out is facilitated by PSLViewer which is pre-installed on the laboratory computer. To connect the software to the CCD cameras, follow the path "Camera" – "Single" – "NTXLaue" (see Fig. 8.4).

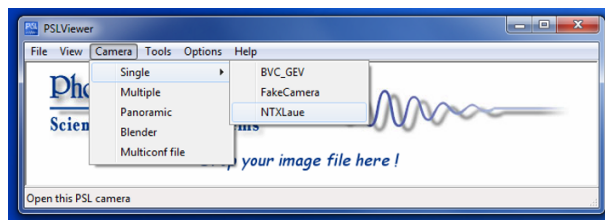


Figure 8.4: PSLViewer start-up screen. The Laue camera can be chosen in the "Camera" menu.

Fig. 8.5 shows the main screen of PSLViewer which consists of a toolbar on the left and the image display on the right. Several instances of the main screen can be opened, e.g. for comparison of different images, however, acquisition of a new image is only possible in the window which has been started as first. Before recording an image, all options in the red marked area in Fig 8.5 can be adjusted. Image acquisition can then be initiated by clicking the "Play" button marked in green. To enhance contrast, maximum intensity corresponding to "white" can be adjusted in the area marked in magenta. The different image options are explained in more detail below.

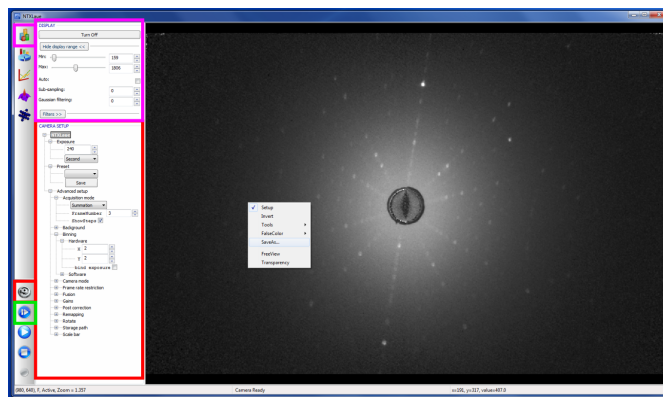


Figure 8.5: Main window of PSLViewer. The toolbar on the left opens several sub-menus. Acquired images are shown on the right.

- Exposure: Spot intensity is given mainly by the exposure time. Greater integrated intensity is always desirable, as it leads to a greater image contrast. It is however limited by the maximum photon count of the CCD chips' pixels. Saturation in the photon count will firstly become noticeable in the centre of an image, since back-scattered intensity is strongest for small angles. Furthermore, long image-acquisition integration times ($t > 600$ s) also amplify the CCDs characteristics, such as dark current and hot pixels, which then requires the use of background subtraction techniques;
- Acquisition mode: Besides the option of taking a single image, several consecutive images can be taken. The respective intensities can either be summed or averaged, which reduces the overall image noise;
- Binning: The hardware binning option adds up the measured intensity of given number of pixels, resulting in a higher sensitivity but smaller resolution. Since higher sensitivity will always allow shorter image-acquisition integration times, binning should be used up to a level that still allows to resolve individual diffraction spots, so that position of the individual spot be unambiguous and neighbouring spots be differentiable. As the spot size depends mainly on the size of the collimated beam, binning should also be chosen with respect to the utilised collimator.

Images can be saved by right-clicking on the image area and choosing "SaveAs...". The standard image format is *.tif which features lossless data in a grey-scale format. Note, however, that the intensity or grey-scale are not saved as an absolute value and thus have to be adjusted each time the image is loaded anew. Within PSLViewer, the *.tif format enables execution of mathematical operations and application of image-enhancement techniques. Furthermore, for a crystal of known symmetry and lattice constants, PSLViewer is also capable of finding and refining the crystal's orientation.

8.5 ANALYSIS SOFTWARE

PSLViewer

The peak symbol in the PSLViewer toolbar (marked magenta in Fig. 8.6) offers the possibility of automatic peak detection. Depending on the parameters given, the image will be evaluated and possible peaks marked with red circles. The threshold parameter determines how large the contrast has to be between the background and the peak in order to be recognised as such. In case peak detection is not desired, the threshold can be set to a high value, e.g. 1000.

The crystal structure symbol (marked blue in Fig. 8.6) opens the simulation and fitting option. In sub-menu "Crystal data", lattice constants, angles, and space group have to be entered in order to simulate a given theoretical pattern. The sub-menu "Instrument data" contains all the parameters associated with the detector (e.g. area of the detector and tilting angles). The only adjustable parameter however is the sample-detector distance and all other parameters should be kept at their preset values.

In order to generate a theoretical Laue pattern for a specific direction, the sub-menu "Find <hkl> spot" will rotate the pattern into the desired direction after pressing the "Find" button.

The pattern can then be rotated or shifted by pressing the left or right mouse button and moving the mouse. Alternatively, the orientation can be directly set by entering orientation angles in the lower part of the menu. A detailed manual is available in the laboratory.

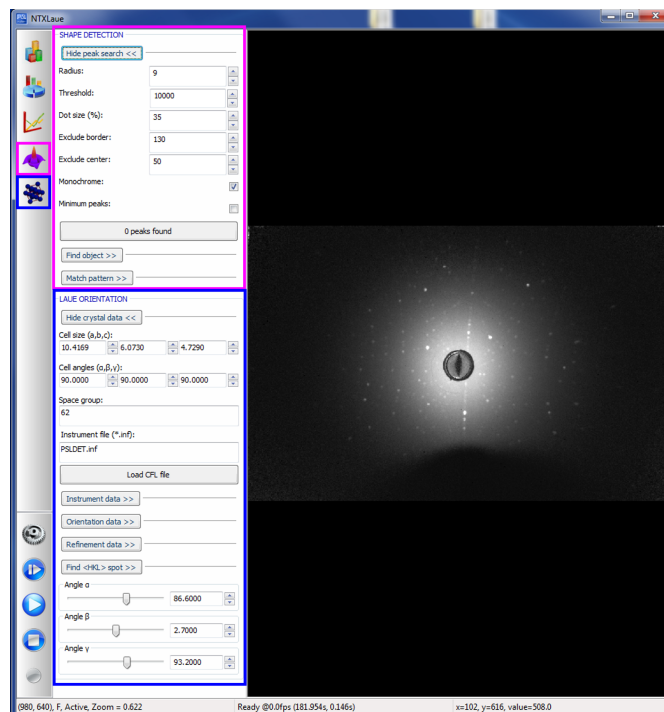


Figure 8.6: Main window of the PSLViewer with shape detection and orientation menu.

CLIP

Alternatively to the techniques offered by PSLViewer, the Cologne Laue Indexation Programme (CLIP) is also available on the laboratory computer. This is recommended for Laue-image analysis, as its system of rotations is more user-friendly than that of PSLViewer, and as it is a standard choice of Laue-image-analysis software in many crystallography laboratories around the world. Furthermore, CLIP is free of charge and can be downloaded also for personal use (see Section 3). Its detailed manual is available in the laboratory. Since CLIP has no direct link to the detector, images have to be imported either as *.png or *.jpeg. To do this, first adjust contrast and brightness with PSLViewer, save the resulting image in a desired format by right-clicking on the PSLViewer's main screen, and then import the image into CLIP using the folder-like button in CLIP's main window. Pressing the screw-wrench-like button in CLIP opens up the detector's geometry settings. Therein, the width and height of the detector (in mm) have already been pre-set, however the sample-detector distance has to be ascertained in the first part of the experimental work. Input of all crystal data is analogue to PSLViewer.

VESTA

VESTA is a three-dimensional real-space visualisation software, ideally suited for visualising microscopic crystal structures of different compounds. It is free of charge and, beyond its availability on the laboratory computer, it can also be downloaded for personal use (see Section 3). It is capable of reading *.cif or *.vesta files, which can be obtained from crystallographic databases. A folder containing CIF (Crystallographic Information File) files of the samples available in the laboratory is saved on the laboratory computer under "Desktop\Mineralien".

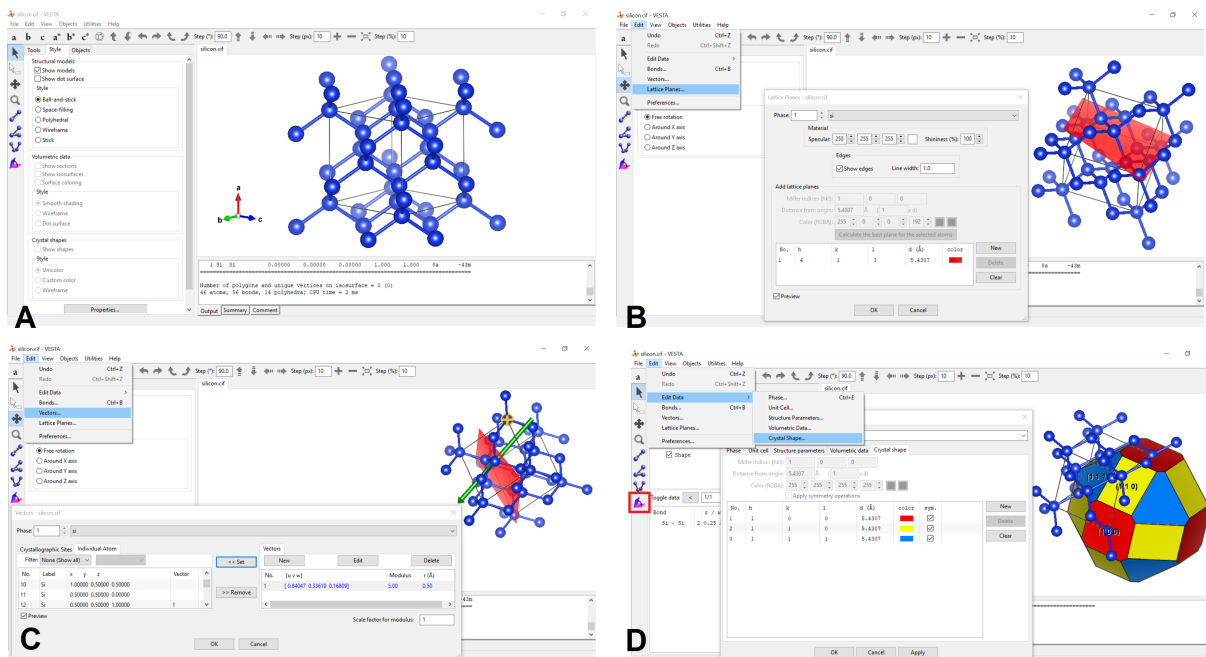


Figure 8.7: Depictions of VESTA's (A) main window; (B) addition of a lattice plane; (C) addition of a vector; (D) generation of a crystal shape.

VESTA offers a comprehensive set of capabilities in visualisation and computation of crystallographic data. Here, we limit ourselves to three functionalities which are required for the completion of current experimental tasks.¹

Fig. 8.7A depicts the main window of the software with a loaded CIF file of silicon. Files can be loaded via the path "File" – "Open", or simply by dragging the desired file into the VESTA window.

In Fig. 8.7B, a lattice plane (4 1 3) has been depicted, located at 5.4307 Å away from the origin. This depiction is achieved by following the path "Edit" – "Lattice Planes", and by inserting the (hkl) values designating the desired plane.

In Fig. 8.7C, an arbitrary vector passing through the silicon atom located at (0.5 0.5 1.0) has been added to the image. This is achieved, in the first step, by following the path "Edit" – "Vectors"; in the second step, by selecting "New" under the vector tab to specify the desired vector, e.g. by means of its [uvw] values; and, in the third step, by clicking "Set" to assign the thus-created vector to a specific atom or atomic site.

¹A full manual is available in the laboratory or can be conveniently accessed via <http://jp-minerals.org/vesta/en/doc.html>.

And lastly, a *crystal shape* of silicon built up of the family of lattice planes $\{1\ 0\ 0\}$, $\{1\ 1\ 0\}$, and $\{1\ 1\ 1\}$ is shown in Fig. 8.7D. To generate a crystal shape, the path "Edit" – "Edit Data" – "Crystal Shape" is followed. Thereafter, planes which are to constitute the crystal shape are selected by clicking "New" (in Fig. 8.7D, the family of planes $\{1\ 0\ 0\}$ – in red, $\{1\ 1\ 0\}$ – in yellow, and $\{1\ 1\ 1\}$ – in blue, have thus been selected).

To depict the crystal shape's desired colour-coding, follow "Style" – "Custom Color" in the main VESTA window. And to display the crystal shape's planes designations, follow "Objects" – "Shape" in the main VESTA window. Clicking on the icon in the red rectangle on the left-hand side of Fig. 8.7D enables the measurement of angles between different planes of the generated crystal shape.

9 EXPERIMENTAL TASKS

9.1 SILICON WAFER

- Choosing one of the silicon wafers available in the laboratory, attach the wafer onto the goniometer by means of the provided playdoh or double-sided tape such that the wafer's planar surface is parallel to the detector. Make thereby use of the L-shaped stand available in the laboratory and ensure that the sample almost touches the tip of the spacer.
- Take a number of Laue images with the help of which you can study (several of) the following effects on the quality of a Laue image:
 1. varying X-ray tube current;
 2. varying X-ray tube voltage;
 3. varying image-acquisition integration time;
 4. varying software binning in the range (1 1)–(3 3).

Creating a new personal folder under "Desktop\Student_Files", save each image as a *.tif and *.png file. Use these images to argue about ideal image-acquisition parameters. Note that in order to enable comparison between different settings, all other parameters must be kept constant (e.g. the setting of the contrast of the acquired Laue images in PSLViewer).

- Produce a high-quality Laue image, employing your refined image-acquisition parameters from the previous task.
- Analyse the latter image with the help of CLIP, thereby obtaining the orientation of the silicon wafer and the sample–detector distance.¹ Save the analysed image as a screenshot bearing information about the crystal structure, the Laue plane and its corresponding stereographic projection, the configuration information, and the reflex information. Make sure that the "Omega", "Chi", "Phi" angles, defining the crystal's orientation, are clearly visible in your screenshot.
- Using the rotary electric motor, rotate the silicon wafer by ca. 15° and take another Laue image. Analyse the image with CLIP as above, and study the effect of the rotation.

¹This and all subsequent image analyses can also be performed with PSLViewer, though this is generally not recommended.

9.2 CRYSTAL OF YOUR CHOICE

- Choosing one of the regularly shaped crystals in the laboratory or using your own crystal, attach the crystal onto the goniometer by means of the provided playdoh or double-sided tape, thereby ensuring that the sample's centre line coincides with the goniometer's centre line. This will allow you to make use of the rotary electric motor in the subsequent task.
- Take Laue images of a number of the crystal's flat faces, using your refined image-acquisition conditions to obtain the images, and the rotary electric motor to align the respective faces parallel to the detector screen.
- Analyse the images by means of CLIP as above, saving the final analyses as screenshots.
- Can any mirror or rotational symmetries be found in the Laue patterns? Are crystal defects visible in the Laue images?
- Take a photographic image or make a sketch of the sample and indicate the crystallographic orientation of the sample's flat faces which you have analysed.
- Calculate the zone axis for a particular set of five planes from one of your Laue images. Depict the chosen planes and your calculated zone axis in VESTA.
- For one of the obtained images, find pixel positions of clearly visible diffraction spots and create an ascii file with the pixel positions in the format "x [TAB] y". This can be done manually or by means of a software (e.g. Matlab or Python). Make sure to quote enough spots so that the crystal's symmetries are identifiable by these spots (around twenty should be sufficient if distributed well over the image). You can also put the hkl index in the third column (x [TAB] y [TAB] hkl) (see example.txt under "Desktop\Mathematica_Routine").
- Generate a stereographic projection of the image by means of the Mathematica file "Laue.nb" which can be found under "Desktop\Mathematica_Routine". For this, copy the file into your working folder, leaving the original intact. Further advice on the implementation of the file is given in the appendix.
- Using low-index crystal planes, build up the crystal shape of your sample in VESTA. Compare the thus-generated crystal shape with the external appearance of your sample. Furthermore, compare the real-space crystal structure as seen in VESTA with the external appearance of your sample. Can you convey reasons from the positions of atoms and the types of bonds (e.g. covalent vs. ionic) why it may be favourable for the crystal to develop the visible faces?
- Use the Wulff net in combination with your stereographic projection to calculate three distinct angles between three planes. Confirm the calculated angles with the help of VESTA. For the latter, you will have to create a crystal shape of your structure composed (at least) of those lattice planes the angle between of which you wish to calculate.

9.3 GENERAL TASKS

- Write down the trigonometric functions which transform a diffraction spot on the detector (i.e. x-,y-pixel) into latitude and longitude of the corresponding pole in a stereographic projection. Inspect the Mathematica script `Laue.nb` for hints.
- Calculate the maximum (hkl) values that are theoretically visible for the applied acceleration voltage. To do so, compare minimum wavelength and minimum interplanar spacing d_{hkl} , and note that depending on the crystal structure only a rough estimate of the maximal (hkl) is possible. Is this in agreement with your experimental observations? What are the sources of the discrepancy?
- How would the observed Laue images change for (i) a tilted detector; (ii) a poorly collimated beam; (iii) a variable sample–detector distance?
- Explain why certain Laue spots appear considerably brighter than their neighbouring spots.
- Discuss possible experimental errors.

A APPENDIX

A.1 SYSTEMATIC EXTINCTION OF REFLEXES

Systematic extinction of reflexes by Bravais type lattice

centering	reflex	condition	centering	reflex	condition
primitive	-	no cancellation			
A-centred	-	$k+l = 2n$	body-centred	hkl	$h+k+l = 2n$
B-centred	-	$h+l = 2n$	face-centred	hkl	$h+k=2n, h+l=2n, k+l=2n$
C-centred	-	$h+k = 2n$	rhombohedral	hkl	$-h+k+l = 3n$

Zonal extinction of reflexes by mirror glide planes

glide plane	position	glide vector	reflex	condition
a	(001)	$a/2$	hk0	$h = 2n$
b	(001)	$b/2$	hk0	$k = 2n$
n	(001)	$a/2 + b/2$	hk0	$h+k = 2n$
d	(001)	$a/4 +/ - b/4$	hk0	$h+k = 4n, h = 2n, k = 2n$
a	(010)	$a/2$	h0l	$h = 2n$
c	(010)	$c/2$	h0l	$l = 2n$
n	(010)	$a/2 + c/2$	h0l	$h+l = 2n$
d	(010)	$a/4 + c/4$	h0l	$h+l = 4n, h=2n, l=2n$
b	(100)	$b/2$	0kl	$k = 2n$
c	(100)	$c/2$	0kl	$l = 2n$
n	(100)	$b/2 + c/2$	0kl	$k+l = 2n$
d	(100)	$b/4 +/ - c/4$	0kl	$k+l = 4n, k = 2n, l = 2n$

Serial extinction of reflexes by screw axes

screw axis	position	reflex	condition	screw axis	position	reflex	condition
$2_1; 4_2; 6_3$	[100]	h00	$h = 2n$	$4_1; 4_3$	[010]	0k0	$k = 4n$
$3_1; 3_2; 6_2; 6_4$	[100]	h00	$h = 3n$	$6_1; 6_5$	[010]	0k0	$k = 6n$
$4_1; 4_3$	[100]	h00	$h = 4n$	$2_1; 4_2; 6_3$	[001]	00l	$l = 2n$
$6_1; 6_5$	[100]	h00	$h = 6n$	$3_1; 3_2; 6_2; 6_4$	[001]	00l	$l = 3n$
$2_1; 4_2; 6_3$	[010]	0k0	$k = 2n$	$4_1; 4_3$	[001]	00l	$l = 4n$
$3_1; 3_2; 6_2; 6_4$	[010]	0k0	$k = 3n$	$6_1; 6_5$	[001]	00l	$l = 6n$

A.2 GENERATION OF STEREOGRAPHIC PROJECTIONS

The provided Mathematica script `Laue.nb` (found under "Desktop\Mathematica_Routine") offers a basic method of calculating longitude (δ) and latitude (γ) from the pixel position of a diffraction spot. The input format is an ascii text file formatted as "x-pixel position" [TAB] "y-pixel position". Multiple diffraction spots have to be written in separate lines and, if desired, additional information, such as the diffraction spot's corresponding (hkl) indices, can be written in the third column. See `example.txt` for a correctly formatted input file under "Desktop\Mathematica_Routine".

Within the Mathematica script, experimental parameters, such as detector-sample distance and resolution (number of pixels), are given in the first block and have to be adjusted. The second block of the script concerns the processing of pixel lists. Here you have to change all the directories in the script to the data directory which contains your lists. Running the script will output several *.txt files containing corresponding latitude and longitude of the spots. The third block outputs a graphic of the stereographic projection, as well as a list of positions projected onto a two-dimensional plane.

Before altering the script, save a copy in your data directory under "Desktop\Student_Files" and leave the original script unchanged.

B FEEDBACK

Please help us make the experiment, and ultimately your experience, better. Your supervisor is always happy to receive verbal feedback – be it positive or negative. To guide your evaluation thoughts, consider addressing the following questions:

- Were you able to follow and comprehend this manual?
- Did you find the performing of the experiment satisfying?
- Did you encounter difficulties in performing the experiment?
- Were you happy with the status of the experimental setup?
- Were you satisfied with your learning experience?
- Were you happy with your supervisor's attitude and aptitude?
- Would you recommend this experiment to your fellow course mates?

Furthermore, do not forget to communicate your feedback via the "Fortgeschrittenen-Praktikum" website. Your time and honesty are greatly appreciated.